Deformable self-propelled domain in an excitable reaction-diffusion system in three dimensions

K. Shitara, T. Hiraiwa, and T. Ohta
Department of Physics, Kyoto University, Kyoto 606-8502, Japan
(Received 24 March 2011; revised manuscript received 16 May 2011; published 21 June 2011)

We derive a set of equations of motion for an isolated domain in an excitable reaction-diffusion system in three dimensions. In the singular limit where the interface is infinitesimally thin, the motion of the center of mass coupled with deformation is investigated near the drift bifurcation where a motionless domain becomes unstable and undergoes migration. This is an extension of our previous theory in two dimensions. We show that there are three basic motions of a domain, straight motion, rotating motion, and helical motion. The last one is a characteristic of three dimensions. The phase diagram of these three solutions is given in the parameter space of the original reaction-diffusion equations.

DOI: 10.1103/PhysRevE.83.066208 PACS number(s): 05.45.−a, 82.40.Ck

I. INTRODUCTION

Self-organized dynamics of domains in reaction-diffusion systems have recently attracted much attention from the viewpoint of nonlinear dynamics [1,2]. Intensive studies employing numerical simulations have revealed fascinating behaviors of domains. For example, Krischer and Mikhailov [3] have shown that a bifurcation from a motionless domain to a propagating domain occurs by changing the system parameter in two dimensions, and the shape of a propagating domain depends on its velocity. Self-replication of domains has been obtained [4], which is qualitatively in agreement with experimental observation [5]. A variety of dynamics of interacting domains has also been discovered [3,6,7]. Theoretically, the domain dynamics has been developed by a singular perturbation method [1,2,8–12].

In a previous paper, Ohkuma and two of the present authors (Ohta and Shitara) studied a single domain dynamics in two dimensions by taking account of shape deformation starting with excitable reaction-diffusion equations [13]. The set of equations for the center of mass and two tensor variables (one is a second-rank tensor and the other is a third-rank tensor) representing shape deformation was derived near the drift instability threshold where a motionless circular domain loses its stability and starts propagating. It was also shown that a straight motion becomes unstable, and the domain undergoes a rotating motion along a circular closed trajectory. This bifurcation was predicted phenomenologically in an earlier study [14], and later, it was obtained by direct numerical simulations of reaction-diffusion equations [15]. Furthermore, the set of equations for the center of mass and the two tensor variables has been solved numerically to show a zig-zag motion, a chaotic motion, and so forth [16]. The interaction among domains has also been investigated [17,18]. Before these studies, there were few theories for deformable self-propulsion [19,20]

In the present paper, we will extend our previous study [13] to three dimensions. The set of time-evolution equations for the velocity of the center of the mass and the second-rank tensor, which represents the elongation of a domain, is derived starting with an excitable reaction-diffusion system with a global coupling. The form of the time-evolution equations is the same as that introduced phenomenologically in three dimensions [21] where a helical motion inherent to three dimensions has been obtained. In the present paper, we derive the phase diagram for straight motion, rotating motion, and helical motion in the parameter space of the original reaction-diffusion equations. Because of complications, the third-rank tensor is not considered in the present paper.

After Ref. [14] was published, we became aware of the fact that the set of time-evolution equations for a deformable self-propelled particle in two dimensions was equivalent with the dynamical system of nonlinear dissipative waves in one dimension under the periodic boundary condition studied by Armbruster *et al*. [22,23] as discussed, to some extent, in Ref. [16]. See also Ref. [15]. We emphasize, however, that such a relationship with the wave dynamics does not exist in self-propelled dynamics of a deformed domain in three dimensions.

The present paper is organized as follows. In Sec. II, we present the reaction-diffusion equations for an activator and an inhibitor with a global coupling. In order to make the present paper self-contained, the mechanism of formation of an isolated domain and its drift instability is briefly reviewed. In Sec. III, we describe the interface dynamics based on the singular perturbation. In Sec. IV, the representation of a deformed domain in three dimensions is given, and the coupled set of time-evolution equations for the center of mass and the tensor variable is obtained. In Sec. V, we carry out order estimation of each term of the equations of motion and derive the stationary solution. The phase diagram for rectilinear motion, rotating motion, and helical motion is given in the parameter space of the original reaction-diffusion system. The modes relevant to the formation of a rotating motion and a helical motion are discussed based on the linear stability of the straight motion and the rotating motion. Summary and discussion are given in Sec. VI. Some of the details in the derivation of the deformation tensor and equations are given in Appendices A–C.

II. EXCITABLE REACTION-DIFFUSION SYSTEM

We start with a coupled set of reaction-diffusion equations for an activator u and an inhibitor v,

$$\tau\varepsilon\frac{\partial u}{\partial t} = \varepsilon^2\nabla^2 u + f\{u,v\} - v, \tag{1}$$

$$\frac{\partial v}{\partial t} = D\nabla^2 v + u - \mu v, \tag{2}$$

where the functional $f\{u,v\}$ is given by

$$f\{u,v\} = -u + H(u - p'\{u,v\}). \tag{3}$$

and $H(x)$ is the Heaviside step function defined as $H(x) = 1$ for $x > 0$ and $H(x) = 0$ for $x < 0$. The functional $p'\{u,v\}$ represents the following global coupling:

$$p' = p + \sigma\left[\int (u+v)d\boldsymbol{r} - W\right], \tag{4}$$

where σ and W are positive constants, $0 < p < 1/2$, and the integral runs over the whole space. The constants τ in Eq. (1) and μ in Eq. (2) are positive and are chosen such that the system is excitable and that a localized stable pulse (domain) solution exists. Inside the domain, the variable u is positive, whereas, outside the domain, u and v asymptotically vanish away from the domain. The parameter ε in Eq. (1) is a measure of the width of the domain boundary. Hereafter, we consider the limit $\varepsilon \to 0$.

The set of Eqs. (1) and (2) with Eqs. (3) and (4) was studied in two dimensions by Krischer and Mikhailov [3]. They investigated dynamics of excitable domains in the vicinity of a drift bifurcation at which a stable stationary domain loses its stability and begins to propagate. They also investigated collision of domains by computer simulations and found that a reflection of a pair of colliding domains occurs near the bifurcation threshold where the propagating velocity is sufficiently small.

The global coupling is necessary in the systems (1) and (2) to prevent a breathing motion in which the radius of a spherical domain undergoes a periodic oscillation [24,25]. It is known that a motionless spherical domain is stable for sufficiently large values of τ and that the drift bifurcation exists for a smaller value of τ than the breathing bifurcation. Therefore, when the value of τ is decreased, the breathing bifurcation generally occurs before the drift bifurcation [3]. If one chooses a sufficiently large value of σ in the global coupling (4), the breathing motion is prohibited as shown below. For $\sigma \to \infty$, Eq. (4) becomes $p' = p$ with

$$\int d\boldsymbol{r}(u+v) = W, \tag{5}$$

and $f\{u,v\}$ is no longer a functional but is given by

$$f(u) = -u + H(u - p). \tag{6}$$

Furthermore, in the limit $\varepsilon \to 0$, Eq. (1) becomes

$$-u + H(u - p) - v = 0. \tag{7}$$

The location of the domain boundary (interface) is defined such that $u = p$ and $u>(<)p$ inside (outside) the domain. From Eq. (7), it is shown that $u + v = 1$ inside the domain, whereas, $u + v = 0$ outside the domain. Therefore, the constraint Eq. (5) means that the volume of an excited domain is conserved and the breathing bifurcation is removed. It is also noted that the drift bifurcation becomes supercritical in the limit $\sigma \to \infty$ [3].

Substituting Eq. (7) into Eq. (2) yields

$$\frac{\partial v}{\partial t} = D\nabla^2 v + H(u - p) - \beta v, \tag{8}$$

where $\beta = 1 + \mu$. The equilibrium solution of a motionless spherical domain with radius R_0 in three dimensions has been obtained in Ref. [8]. Noting the relation that $H(u - p) = H(R_0 - r)$, the equilibrium solution $v = \bar{v}$ from Eq. (8) is given for $0 < r < R_0$ by

$$\bar{v} = \frac{1}{\beta}\left[1 - \left(1 + \frac{R_0}{\xi}\right)e^{-R_0/\xi}\frac{\sinh(r/\xi)}{r/\xi}\right], \tag{9}$$

and for $r > R_0$ by

$$\bar{v} = \frac{1}{\beta}\left[\frac{R_0}{\xi}\cosh\left(\frac{R_0}{\xi}\right) - \sinh\left(\frac{R_0}{\xi}\right)\right]\frac{e^{-r/\xi}}{r/\xi}, \tag{10}$$

where

$$\xi = \sqrt{\frac{D}{\beta}}. \tag{11}$$

The equilibrium solution $\bar{u}$ is given by the relation $\bar{u} = H(R_0 - r) - \bar{v}$ in Eq. (7). From Eqs. (9) and (10), we note that the inhibitor v changes gradually in space with the characteristic length ξ, whereas, the activator u is discontinuous at $r = R_0$ for $\varepsilon \to 0$. It is noted that, when the global coupling (5) is present, the radius R_0 of an excited domain is a parameter imposed externally provided that $W = 4\pi R_0^3/3$.

In the following sections, we will show that a motionless isolated spherical domain becomes unstable by changing the parameter τ, and we will derive the time-evolution equations. Before entering the mathematical analysis, we will explain the previous results [8,10] as intuitively as possible. First of all, why is an isolated domain stable for sufficiently large values of τ? Suppose that, initially, the activator is finite and positive for a certain spherical area, and the inhibitor is zero anywhere. When τ is large, the activator is slow, and, hence, the inhibitor is produced quickly by the reaction term $+u$ in Eq. (2). This, in turn, tends to diminish the activator because of the $-v$ term in Eq. (1). However, when the diffusion constant of the inhibitor is much larger than that of the activator, the produced inhibitor rapidly diffuses away from the region where the activator is finite. Therefore, if a balance between the production and the diffusion of the inhibitor occurs, a localized stationary domain is stable. Another way to understand existence of a stable localized excited domain for large values of τ is as follows. When the inhibitor relaxes rapidly, one may set $\partial v/\partial t = 0$. Therefore, v is given by $v = [-D\nabla^2 + \mu]^{-1}u$. Substituting this into Eq. (1), one notes that, when D is large enough, there is a Coulomb-type repulsive interaction for the field u. This is a general mechanism for the formation of spatially periodic structures, including the infinite period, i.e., the case of an isolated domain [26,27].

The second question is why an isolated motionless domain becomes unstable by decreasing the value of τ. Suppose a spherical domain with a sharp interface of u and with a diffuse concentration profile of v, which is a decreasing function of the distance from the center of mass. If the profile of u is slightly translated to the right, as shown in Fig. 1, the local concentration of the inhibitor quickly adjusts by the reaction term when τ is sufficiently large so that the profile of u returns to the original one. However, when τ is small, the time evolution of v becomes slow so that v cannot follow the local change of the activator. Since the concentration profile

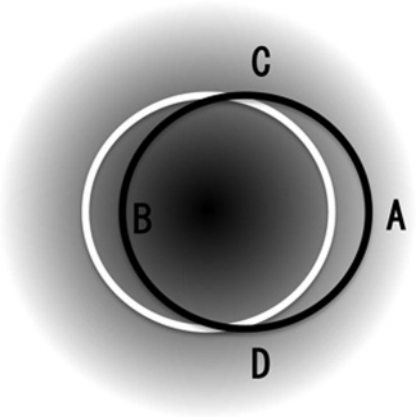

FIG. 1. An imbalance in the spatial profiles between u and v causes a further drift of the excited domain. The white circle and the gray domain indicate the interface of the variable u and the diffuse profile of v, respectively, in the motionless state. If the interface drifts to the right as shown by the black circle, the inhibitor is smaller than the equilibrium value near points A, C, and D, whereas, it is larger than the equilibrium near point B, and, hence, the excited domain tends to drift further to the right expanding to the C and D directions unless the recovering of v is not sufficiently rapid.

of v is a decreasing function of the distance from the center, a slight translation of u causes an imbalance between u and v such that the translation is enhanced. This is the mechanism of the drift bifurcation that occurs by decreasing the parameter τ.

The above consideration implies that the difference in the diffusion constants and the difference in the characteristic times between the activator and the inhibitor are essential for the formation of an isolated excited domain and the drift bifurcation, which is insensitive to the details of the time-evolution equations.

III. INTERFACE EQUATION OF MOTION

In order to take account of the spatial variation of u near the interface at $r = R_0$, one must magnify the space coordinate as $r' = r/\varepsilon \sim O(1)$. In this length scale, the spatial variation of v is negligible, and the value of v in Eq. (1) can be replaced by the value at the interface $v(\boldsymbol{r},t) \equiv w$. For a given value of w, from Eq. (1), one can readily obtain the equation of motion for a smoothly deformed interface as [8]

$$\tau V = \varepsilon K + \tau c(w) + L, \tag{12}$$

where V is the normal component of the velocity directed from the inside to the outside of a domain and K is the mean curvature defined such that it is positive when the center of the curvature is outside the excited domain. The second term in Eq. (12) is the velocity for a flat interface and is related to w as [28]

$$\frac{c\tau}{[(c\tau)^2+4]^{1/2}} = 1 - 2p - 2w. \tag{13}$$

The value of w is determined by solving Eq. (2) or (8) for a given interface configuration. The last term L in Eq. (12) is a Lagrange multiplier for the constraint of the domain volume conservation given by Eq. (5) and is determined by the condition

$$\int d\omega\, V(\omega) = 0, \tag{14}$$

where ω specifies the position on the interface and $d\omega$ is the infinitesimal area of the interface and the integral runs over the interface.

We consider an isolated deformed domain. The velocity of the center of mass $\boldsymbol{\rho}(t)$ is given by

$$\dot{\boldsymbol{\rho}} = \frac{1}{\Omega}\int d\omega\, V(\theta,\phi)\boldsymbol{R}(\theta,\phi), \tag{15}$$

where the dot indicates the time derivative, θ is the polar angle, ϕ is the azimuthal angle in the spherical coordinate, and $d\omega = R^2 d\theta\, d\phi \sin\theta$. The constant Ω is the volume of the domain, and

$$\boldsymbol{R}(\theta,\phi) = R(\theta,\phi)\boldsymbol{e}_r, \tag{16}$$

with the radial unit vector $\boldsymbol{e}_r$. Deformations of a domain around a spherical shape are written as

$$R(\theta,\phi,t) = R_0 + \delta R(\theta,\phi,t), \tag{17}$$

where

$$\delta R(\theta,\phi,t) = \sum_{\ell,m} c_{\ell m}(t) Y_\ell^m(\theta,\phi). \tag{18}$$

The spherical harmonics $Y_\ell^m(\theta,\phi)$ is defined by

$$Y_\ell^m(\theta,\phi) = \sqrt{\frac{(2\ell+1)(\ell-|m|)!}{4\pi(\ell+|m|)!}} P_\ell^{|m|}(\cos\theta) e^{im\phi}, \tag{19}$$

where $P_\ell^m(\cos\theta)$ is the associated Legendre function. Since the translational motion of a domain has been incorporated in the variable $\boldsymbol{\rho}$, the modes $c_{1m}(m = \pm 1)$ should be removed from the expansion in Eq. (18).

The normal velocity V and the mean curvature K in Eq. (12) are represented, respectively, by

$$V(\boldsymbol{r},t) = -\frac{1}{|\nabla U|}\frac{\partial U}{\partial t}\bigg|_{U=0}, \tag{20}$$

$$K(\boldsymbol{r},t) = -\nabla\cdot\left(\frac{\nabla U}{|\nabla U|}\right)\bigg|_{U=0}, \tag{21}$$

where

$$U(\boldsymbol{r},t) = r - R(\theta,\phi,t). \tag{22}$$

Up to the first order of the deformation δR, these are calculated as [29]

$$V(\theta,\phi,t) = \dot{\boldsymbol{\rho}}\cdot\boldsymbol{n} + \sum_{\ell,m}\dot{c}_{\ell m}(t) Y_\ell^m(\theta,\phi), \tag{23}$$

$$K(\theta,\phi,t) = -\frac{2}{R_0} - \frac{1}{R_0^2}\sum_{\ell,m}(\ell+2)(\ell-1)c_{\ell m}(t) Y_\ell^m(\theta,\phi). \tag{24}$$

In order to express a biaxial deformation of domain, we introduce the following second-rank tensor:

$$S_{ij} = \sum_{m=1}^{3} q_m n_i^{(m)} n_j^{(m)}, \tag{25}$$

where the moduli q_1, q_2, and q_3 satisfy $q_1 + q_2 + q_3 = 0$ [30]. The unit vectors $\boldsymbol{n}^{(1)}$, $\boldsymbol{n}^{(2)}$, and $\boldsymbol{n}^{(3)}$ are orthogonal to each other

and specify the direction of a rigid body. The tensor defined by Eq. (25) is symmetric and traceless. In two dimensions, there are two orthogonal unit vectors $\boldsymbol{n}^{(1)}$ and $\boldsymbol{n}^{(2)}$ with $q_1 + q_2 = 0$, and S_{ij}, given by Eq. (25), is equivalent with $S_{ij} = 2q_1[n_i n_j - (1/2)\delta_{ij}]$. The representation of deformations (25) should be compared with the expansionlike Eq. (18), which is in terms of the spherical harmonics in three dimensions but in terms of Fourier modes in two dimensions, and, therefore, the expansion strongly depends on the dimensionality of space. Therefore, the representation of a deformed domain, in terms of S_{ij}, is more general and convenient rather than in terms of the coefficients $c_{\ell m}$ in Eq. (18). Hence, we will derive the equation for S_{ij}. In order to achieve this, one needs the relation between the coefficients $c_{\ell m}$ and the tensor S_{ij}. The details of the derivation are described in Appendix A. The final results are given by

$$\begin{aligned} S_{11} &= (3/2)^{1/2}(c_{22} + c_{2-2}) - c_{20}, \\ S_{12} &= S_{21} = i(3/2)^{1/2}(c_{22} - c_{2-2}), \\ S_{13} &= S_{31} = (3/2)^{1/2}(c_{21} + c_{2-1}), \\ S_{22} &= -(3/2)^{1/2}(c_{22} + c_{2-2}) - c_{20}, \\ S_{23} &= S_{32} = i(3/2)^{1/2}(c_{21} - c_{2-1}), \\ S_{33} &= -(S_{11} + S_{22}). \end{aligned} \tag{26}$$

These relations enable us to draw the shape of a domain by solving the time-evolution equation for the tensor S_{ij}.

IV. EQUATION OF MOTION FOR $\boldsymbol{\rho}(t)$ AND S_{ij}

In this section, we derive the time-evolution equation of the center of mass of a domain $\boldsymbol{\rho}$ and the tensor S_{ij}. When the motion of the interface is slow compared with the relaxation rate of the inhibitor, one may deal with the term $\partial v/\partial t$ in Eq. (8) as a perturbation so that its asymptotic solution can be written as

$$v(\boldsymbol{r},t) = GH - G^2\frac{\partial H}{\partial t} + G^3\frac{\partial^2 H}{\partial t^2} - G^4\frac{\partial^3 H}{\partial t^3} + \cdots, \tag{27}$$

where G is defined through the relation

$$(-D\nabla^2 + \beta)G(\boldsymbol{r} - \boldsymbol{r}') = \delta(\boldsymbol{r} - \boldsymbol{r}'), \tag{28}$$

and the abbreviation such that $GA = \int d\boldsymbol{r}' G(\boldsymbol{r} - \boldsymbol{r}')A(\boldsymbol{r}')$ has been used. For an isolated domain, the Fourier transform of $H(u - p) = H(R - |\boldsymbol{r} - \boldsymbol{\rho}|)$ is given by

$$H_q = \int_{|\boldsymbol{r}-\boldsymbol{\rho}|<R} d\boldsymbol{r}\ \exp(-i\boldsymbol{q}\cdot\boldsymbol{r}). \tag{29}$$

Here, the Fourier transformation is defined by

$$A(\boldsymbol{r},t) = \int_{\tilde{q}} A_{\boldsymbol{q}}(t)e^{i\boldsymbol{q}\cdot\boldsymbol{r}}, \tag{30}$$

$$A_{\boldsymbol{q}}(t) = \int d\boldsymbol{r}\, A(\boldsymbol{r},t)e^{-i\boldsymbol{q}\cdot\boldsymbol{r}}, \tag{31}$$

where $\int_{\tilde{q}} = \int d\boldsymbol{q}/(2\pi)^d$, with d as the dimensionality of space.

From Eqs. (12), (13), and (27), the following time-evolution equation for the center of mass $\boldsymbol{\rho}$ is derived:

$$m\ddot{\rho}_i + \tfrac{1}{2}(\tau - \tau_c)\dot{\rho}_i + g\dot{\rho}_i|\dot{\boldsymbol{\rho}}|^2 = -a\dot{\rho}_j S_{ji}, \tag{32}$$

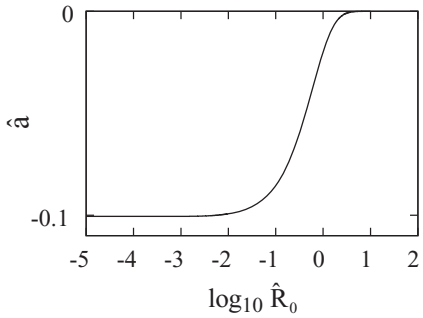

FIG. 2. The coefficient $\hat{a} \equiv aD^2/R_0^2$ as a function of $\hat{R}_0 = R_0/\xi$. Note, from Eqs. (36), (B31), and (B40), that $\hat{a}$ is a function only of $\hat{R}_0$, independent of any other parameters in the original reaction-diffusion equations (1) and (2) with Eqs. (3) and (4).

where the repeated indices imply summation and

$$m = \frac{4R_0^2}{\pi}\int_0^\infty dq\, q^2 G_q^3 j_1(qR_0)^2, \tag{33}$$

$$\tau_c = \frac{8R_0^2}{\pi}\int_0^\infty dq\, q^2 G_q^2 j_1(qR_0)^2, \tag{34}$$

$$g = \frac{12R_0^2}{5\pi}\int_0^\infty dq\, q^4 G_q^4 j_1(qR_0)^2 - \frac{3\tau^3}{80}, \tag{35}$$

$$a = 2(a_1 + a_2), \tag{36}$$

and a_1 and a_2 are given by Eqs. (B31) and (B40), respectively, in Appendix B where the details of the derivation of Eq. (32) are given. G_q is the Fourier transform of G and is given by

$$G_q = \frac{1}{D(q^2 + 1/\xi^2)}. \tag{37}$$

The function $j_1(x)$ is the spherical Bessel function defined by Eq. (B8). The coefficient m is positive, and g is shown to be positive for $\tau \sim \tau_c$. Therefore, Eq. (32) indicates a drift bifurcation at $\tau = \tau_c$ below which a stable stationary spherical domain becomes unstable and begins propagating at the velocity $|\dot{\boldsymbol{\rho}}|^2 = (\tau_c - \tau)/(2g)$. The coefficient a is evaluated numerically and is found to be negative as shown in Fig. 2. When $\hat{R}_0 \to 0$, one obtains an analytical expression $\hat{a} = -2/(5\sqrt{5\pi})$. The fact that $a < 0$ has a deep meaning will be described at the end of this section.

As mentioned above, Eq. (32) admits a supercritical drift bifurcation. However, we remark that a bifurcation from a motionless domain to a propagating domain is not restricted to excitable systems. For instance, a droplet in a binary fluid undergoes self-propulsion due to a Marangoni effect. That is, if there is a third component that affects the surface tension of the droplet, the inhomogeneity of the surface tension causes a translational motion of the droplet when the Marangoni effect exceeds the drag force. In fact, an equation similar to the second and the third terms on the left hand side of Eq. (32) has been derived starting with the hydrodynamic equation with a suitable boundary condition at the droplet surface [31]. This implies that the left hand side is a generic structure of the drift bifurcation independent of the details of the systems concerned.

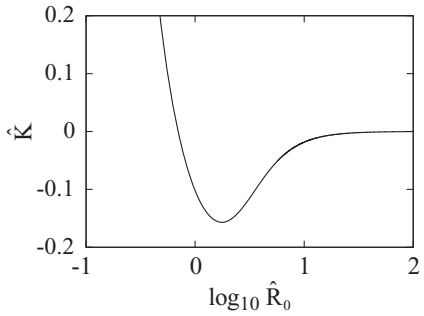

FIG. 3. The coefficient $\hat{K} \equiv K\xi$ as a function of $\hat{R}_0 = R_0/\xi$ for $\varepsilon = 1.25 \times 10^{-2}$, $\mu = 1.0$, and $D = 1.0$.

The time-evolution equation of the tensor S_{ij} is also derived from Eqs. (12), (13), and (27) as

$$\Gamma \frac{d}{dt} S_{ij} = -K S_{ij} + b \left(\dot{\rho}_i \dot{\rho}_j - \frac{1}{3} \delta_{ij} |\dot{\boldsymbol{\rho}}|^2 \right), \tag{38}$$

where

$$\Gamma = \tau - \frac{8B_2}{\pi}, \tag{39}$$

$$K = \frac{4\varepsilon}{R_0^2} + \frac{8A_2}{\pi}, \tag{40}$$

$$b = -\frac{32D_1}{\sqrt{5\pi}}. \tag{41}$$

The details of the derivation are given in Appendix C. The coefficients A_ℓ, B_ℓ, and D_ℓ are given by Eqs. (C9), (C10), and (C11), respectively. In the vicinity of the bifurcation $\tau \sim \tau_c$ with τ_c given by Eq. (34), the coefficient Γ is positive. The coefficient K becomes negative for large values of R_0 as shown in Fig. 3 indicating an instability of a motionless spherical domain [8]. As described at the end of Sec. II, there is a Coulomb-type repulsive interaction for the activator. Hence, this shape instability, by increasing the radius, is equivalent mathematically with the Rayleigh instability of a charged droplet. Here, we restrict ourselves to the case of $K > 0$.

The coefficient b is negative for $0 < \hat{R}_0 < \infty$ as shown in Fig. 4, in particular, $\hat{b} = -(16/35)\sqrt{\pi/5}$ for $\hat{R}_0 \to 0$. In two dimensions, the domain undergoing a straight motion is elongated perpendicularly to the migration velocity [14]. In the next section, we will show that the situation is the same in

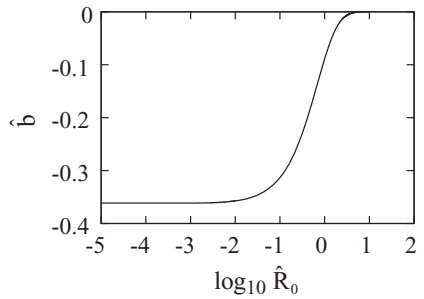

FIG. 4. The coefficient $\hat{b} \equiv bD^3/R_0^4$ as a function of $\hat{R}_0 = R_0/\xi$. Note that $\hat{b}$ is a function only of $\hat{R}_0$, independent of any other parameters of Eqs. (1) and (2).

three dimensions. The reason for the perpendicular elongation is that the value of the inhibitor in the region indicated by C and D in Fig. 1 is smaller than the equilibrium value so that the excited domain tends to expand in these areas.

As mentioned above, the coefficient b should be negative in the excitable reaction-diffusion systems (1) and (2). We show that the fact that the other coefficient a is also negative is related to the fact that the excitable system is nonvariational. It is noted that, if $ab < 0$, i.e., if $a > 0$ and $b < 0$, Eqs. (32) and (38) have a Lyapunov function given by

$$H_{Ly} = -\frac{\gamma''}{2} |\dot{\boldsymbol{\rho}}|^2 + \frac{g''}{4} |\dot{\boldsymbol{\rho}}|^4 + \frac{a''}{2} S_{ij} \dot{\rho}_i \dot{\rho}_j + \frac{K'}{2} S_{ij} S_{ij}, \tag{42}$$

where g'', a'', and K' must be positive. From this, one obtains

$$m \ddot{\rho}_i = -L_1 \frac{\partial H_{Ly}}{\partial \dot{\rho}_i}, \tag{43}$$

$$\Gamma \frac{d}{dt} S_{ij} = -L_2 \frac{\partial H_{Ly}}{\partial S_{ij}} + T, \tag{44}$$

where L_1 and L_2 are positive and T is the Lagrange multiplier to ensure that S_{ij} is traceless. If one sets $(\tau_c - \tau)/2 = L_1 \gamma''$, $g = g'' L_1$, $a = a'' L_1/2 > 0$, $K = L_2 K'$, and $b = -a'' L_2/2 < 0$, Eqs. (43) and (44) are equivalent with Eqs. (32) and (38). This property generally contradicts the fact that the original reaction-diffusion systems (1) and (2) are nonvariational.

Finally, we comment about why the absolute value of coefficients a and b is a decreasing function of the domain radius R_0. The coupling between the migration velocity and the deformation originates from the nonlocal interaction between two points on the interface, which is mediated by the diffusion of the inhibitor. Since any pair of points on the interface becomes distant, on average, when R_0 is increased, keeping other length unchanged, the effect of the interaction decreases so that the magnitude of coefficients a and b becomes low.

V. ORDER ESTIMATION AND STATIONARY SOLUTIONS

In this section, we discuss justification of the approximations employed in the derivations of the time-evolution equations (32) and (38). After that, we derive the stationary solutions of a domain. We are considering the situation in the vicinity of the supercritical drift bifurcation $\tau = \tau_c$ so that $\delta = \tau - \tau_c$ can be regarded as a small parameter. It is found that all the terms of Eq. (32) are on the order of $\delta^{3/2}$ since $\dot{\boldsymbol{\rho}} \sim O(\delta^{1/2})$ and time is scaled as $\hat{t} = t\delta$ and $S \sim O(\delta)$ as can be seen from the first and second terms in Eq. (38). For consistency with these estimations, we have ignored several terms in Eq. (32) that are higher in order of δ, such as $d^2\dot{\boldsymbol{\rho}}/dt^2 \sim O(\delta^{5/2})$ and $SS\dot{\boldsymbol{\rho}} \sim O(\delta^{5/2})$. On the other hand, the terms on the right hand side of Eq. (38) are on the order of $O(\delta)$, whereas, $dS/dt \sim O(\delta^2)$ and all other terms, which are ignored, are higher order. Therefore, up to the leading order, the time derivative of S should be ignored. This is not surprising since, for $\delta \to 0$, the center of mass is a slow variable, but the deformations around a spherical shape are not generally slow and might be eliminated adiabatically. This fact does not cause any difficulties in the study of the stationary shape of the domain. However, if the deformation tensor is also a slow variable such that the coefficient $\Gamma \sim O(\delta^{-1})$, we have

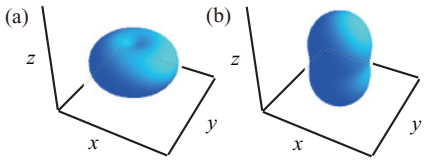

FIG. 5. (Color online) Stationary shape of a domain moving along the z axis. (a) The domain is elongated to the direction perpendicular to the velocity when $b' < 0$, and (b) the domain is elongated to the direction parallel to the velocity when $b' > 0$.

to retain the term $\Gamma \times dS/dt$. As a result, not only a straight motion, but also other types of motions appear as will be shown below.

In order to investigate the stationary solutions of a propagating domain, we represent the velocity of the center of mass as $\dot{\boldsymbol{\rho}} = |\dot{\boldsymbol{\rho}}|\boldsymbol{u}$. It is convenient to introduce the inner product of the principal axes of the deformed domain and the normal unit vector $\boldsymbol{u}$ as

$$P_i \equiv \boldsymbol{n}^{(i)} \cdot \boldsymbol{u} \qquad (i = 1,2,3). \tag{45}$$

Note that the following condition should be satisfied:

$$P_1^2 + P_2^2 + P_3^2 = 1. \tag{46}$$

The center-of-mass velocity can be represented as $\dot{\boldsymbol{\rho}} = \dot{\rho} P_1 \boldsymbol{n}^{(1)} + \dot{\rho} P_2 \boldsymbol{n}^{(2)} + \dot{\rho} P_3 \boldsymbol{n}^{(3)}$. We may assume, without loss of generality, that $P_1 \geqslant P_2 \geqslant P_3$. In order to represent a biaxial deformation, we define

$$\eta \equiv q_2 - q_3. \tag{47}$$

Equations (32) and (38) are written in terms of these variables as [21]

$$\ddot{\rho} = \gamma\dot{\rho} - \dot{\rho}^3 - a'\dot{\rho}\left(q_1 P_1^2 - Q^- P_2^2 - Q^+ P_3^2\right), \tag{48}$$

$$\frac{dq_1}{dt} = -\kappa q_1 + b'\dot{\rho}^2\left(P_1^2 - \frac{1}{3}\right), \tag{49}$$

$$\frac{d\eta}{dt} = -\kappa\eta + b'\dot{\rho}^2\left(P_2^2 - P_3^2\right), \tag{50}$$

$$\frac{dP_1}{dt} = \frac{2b'\dot{\rho}^2}{3q_1 - \eta} P_1 P_2^2 + \frac{2b'\dot{\rho}^2}{3q_1 + \eta} P_1 P_3^2 + a' P_1\left[q_1\left(P_1^2 - 1\right) - Q^- P_2^2 - Q^+ P_3^2\right], \tag{51}$$

$$\frac{dP_2}{dt} = -\frac{2b'\dot{\rho}^2}{3q_1 - \eta} P_2 P_1^2 + \frac{b'\dot{\rho}^2}{\eta} P_2 P_3^2 + a' P_2\left[q_1 P_1^2 - Q^-\left(P_2^2 - 1\right) - Q^+ P_3^2\right], \tag{52}$$

$$\frac{dP_3}{dt} = -\frac{2b'\dot{\rho}^2}{3q_1 + \eta} P_3 P_1^2 - \frac{b'\dot{\rho}^2}{\eta} P_3 P_2^2 + a' P_3\left[q_1 P_1^2 - Q^- P_2^2 - Q^+\left(P_3^2 - 1\right)\right], \tag{53}$$

where $Q^\pm = q_1/2 \pm \eta/2$, $\gamma = (\tau_c - \tau)g/(2m^2)$, $a' = (ag)/m^2$, $\kappa = (Kg)/(\Gamma m)$, and $b' = (bm)/(g\Gamma)$. Here, we have rescaled the time as $t = (g/m)t'$, and we have dropped the prime in t' in Eqs. (48)–(53). From Eqs. (48)–(53), one obtains the stationary solution of a straight motion as

$$\dot{\rho}_s^2 = \frac{3\kappa\gamma}{3\kappa + 2a'b'}, \tag{54}$$

$$q_{1,s} = \frac{2b'}{3\kappa}\dot{\rho}_s^2, \tag{55}$$

$$P_{1,s}^2 = 1, \tag{56}$$

and $\eta_s = P_{2,s} = P_{3,s} = 0$. From Eq. (55), one notes that the sign of the constant b' determines the sign of $q_{1,s}$. As shown in Fig. 4, the constant b' is negative. Therefore, the domain undergoing a straight motion is elongated perpendicularly to the propagating velocity as shown in Fig. 5(a).

The straight motion becomes unstable at the threshold given by [21]

$$\gamma = \frac{\kappa^2}{a'b'} + \frac{2}{3}\kappa, \tag{57}$$

This bifurcation is indicated by the broken line in Fig. 6. Beyond the threshold, a rotating motion appears, whose solution is obtained as

$$\dot{\rho}_r^2 = \frac{3\kappa(2\gamma - \kappa)}{6\kappa + a'b'}, \tag{58}$$

$$P_\pm^2 = \frac{1}{2} \pm \frac{\kappa}{2}\sqrt{\frac{6\kappa + a'b'}{a'b'(6\kappa\gamma - 3\kappa^2)}}, \tag{59}$$

$$q_{1,r} = \frac{b'\dot{\rho}_r^2(P_+^2 - 1/3)}{\kappa}, \tag{60}$$

$$\eta_r = \frac{b'\dot{\rho}_r^2 P_-^2}{\kappa}, \tag{61}$$

where $P_\pm$ are the stationary solutions of Eqs. (51) and (52). One may set $P_1 = P_+$, $P_2 = P_-$, and $P_3 = 0$ because of the conditions $P_1 \geqslant P_2 \geqslant P_3$ and because the motion is confined to a plane. By decreasing the value of κ further, the rotating motion loses its stability, and the helical motion becomes stable. The threshold is given by [21]

$$\gamma = \frac{3\kappa^2}{a'b'} + \kappa, \tag{62}$$

which is shown by the dotted line in Fig. 6. The analytical expression of the helical motion has not been obtained. A rotating motion and a helical motion obtained numerically from Eqs. (48)–(53) are shown in Fig. 7.

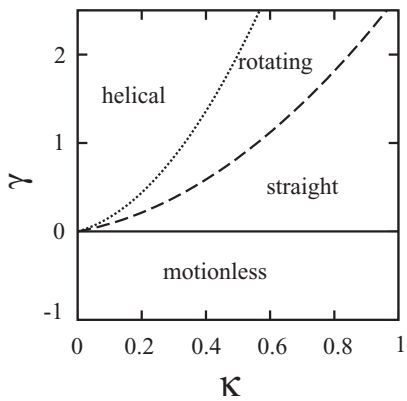

FIG. 6. Phase diagram on the γ-κ plane for $a' = -1.0$ and $b' = -0.5$. The solid line indicates the supercritical bifurcation such that a motionless spherical domain becomes unstable. The broken line and dotted line are given by Eqs. (57) and (62), respectively.

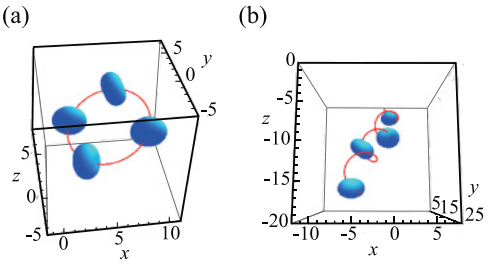

FIG. 7. (Color online) (a) Rotating motion for $\gamma = 0.5$ and $\kappa = 0.3$, and (b) helical motion for $\gamma = 0.5$ and $\kappa = 0.2$.

The parameters γ and κ in Eqs. (48)–(50) are most important for the dynamics of a domain. When the relaxation rate of deformation or the rigidity of a domain κ is much larger than γ, the deformation quickly follows the center-of-mass velocity, and, hence, no instability of the rectilinear motion occurs. However, if the normal direction of the pancakelike domain deviates from the migration direction, it cannot be restored immediately for smaller values of the relaxation rate κ. This results in an instability of the straight motion. The linear stability analysis of the straight motion in Eqs. (48)–(53) indicates that, in this case, the unstable modes are P_2 and P_3, which are 2 degrees of freedom perpendicular to the migration velocity [21]. Actually, these two variables behave as $P_2 \sim P_3 \propto \exp(\lambda t)$ where

$$\lambda = \frac{-\kappa^2 - 2a'b'\kappa/3 + a'b'\gamma}{\kappa + 2a'b'/3}. \tag{63}$$

The bifurcation threshold (57) has been obtained from this. In the case of a rotating motion, two variables P_1 and P_2 are nonzero specifying the plane of the rotation. The linear stability tells us that the third component P_3, which is the coordinate perpendicular to the plane, becomes unstable at the threshold given by Eq. (62).

The bifurcation thresholds given by Eqs. (57) and (62) depend on a', b', and κ. These are the coefficients of Eqs. (32) and (38) that are given in terms of the parameters in the original reaction-diffusion equations (1) and (2) with Eqs. (3) and (4). The most relevant parameters in Eqs. (1) and (2) with $\epsilon \to 0$ are the radius of domain R_0, the diffusion length of the inhibitor ξ, and the characteristic time τ of the activator. Since R_0 is a parameter controlled externally, and the coefficient τ is the drift-bifurcation parameter, it is convenient to choose $\hat{R}_0$ and

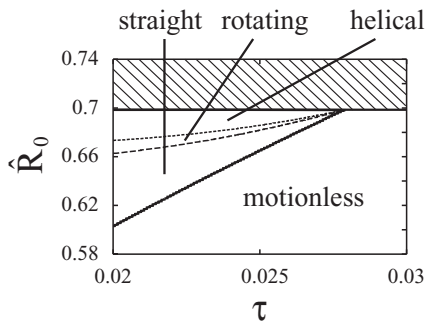

FIG. 8. Phase diagram on the $\hat{R}_0$-τ plane for $\varepsilon = 1.25 \times 10^{-2}$, $\mu = 1.0$, and $D = 1.0$. In the region indicated by the tilted lines, the coefficient K is negative.

τ as fundamental parameters. The phase diagram in Fig. 6 can be transformed on the plane of $\hat{R}_0$ and τ as displayed in Fig. 8, where the parameter regions for the motionless state, the straight motion, the rotating motion, and the helical motion are explicitly given. As can be seen from Fig. 3, the value of K decreases rapidly near $K = 0$. This is the reason why the region of the rotating and helical motions is rather narrow in Fig. 8.

VI. SUMMARY AND DISCUSSION

We have studied the coupling of translational motion and shape deformation of a domain in an excitable reaction-diffusion system in three dimensions. The set of time-evolution equations (32) and (38) has been derived by the singular perturbation method. Coefficients a and b are found to be negative. This implies that the deformed shape of a steady propagating domain in Eqs. (1) and (2) takes the form shown in Fig. 5(a). We have also shown that straight motion, rotating motion, and helical motion, predicted in Ref. [21], should occur in this reaction-diffusion system.

Since the form of Eqs. (32) and (38) is quite general, one may expect that helical motion as well as rotating motion should be observed in three dimensions in excitable reaction-diffusion systems. The fundamental properties employed in the derivation of Eqs. (32) and (38) are as follows; (1) An excited domain has a sharp interface, (2) the diffusion of the inhibitor is much larger than the activator, and (3) the characteristic time of the interface motion of an excited domain is small compared with that of the inhibitor. We expect that, if these conditions are satisfied, the dynamics predicted here are observed. As mentioned in Sec. I, a rotating motion has been obtained by numerical simulations of another reaction-diffusion system in two dimensions [15]. Therefore, extension of this numerical study to three dimensions is quite interesting to explore more varieties of dynamics.

Many experiments of excitable systems, such as gas discharge [2] and chemical reactions [4,5,32] are in two dimensions or quasi-two dimensional where a typical domain size is much larger than the thickness of the system. Therefore, it is unlikely to realize a helical motion experimentally in these systems. The bifurcation neither of the rectilinear-to-rotating motion nor of the rotating-to-helical motion has been observed experimentally. Probably, experiments of the self-propulsion of chemically reacting oily droplets with micrometer size [33,34] are more suitable since those are carried out in three dimensions. The oily droplets obey the hydrodynamic equations with Marangoni effects. Although the time-evolution equations (32) and (38) have not been derived in such a case, we believe that the equations with the same structure hold with the coefficients depending on the viscosities of the oil droplets and the surrounding fluid and the concentration-dependent interfacial tension.

Finally, we comment on the relation between the present results and the helical motions observed in many microorganisms. For example, *Listeria* is propelled along a helical trajectory by forming a comet tail of actin filament [35]. Sperm cells swim with a helical motion by generating a bending wave along a flagellum [36]. In the theoretical analysis of helical motions in these biological systems, not

only a propulsive force for translation, but also a torque for spinning are considered [37,38]. On the other hand, our system, governed by Eqs. (32) and (38), does not possess any intrinsic spinning degrees of freedom. Therefore, it is not appropriate to compare the helical motion obtained in the present paper with those of the micro-organisms. This provides us with an interesting problem for generalizing Eqs. (32) and (38) coupled to an angular variable (tensor) to represent spinning motions. This is not trivial even in two dimensions since an interplay between rotating motion (orbital revolution) and spinning motion causes complex dynamics [39]. We will publish these studies elsewhere in the near future.

ACKNOWLEDGMENTS

We are grateful to Dr. T. Ohkuma for his contribution at the early stage of this work. We would also like to thank Professor H.-Y. Chen and Dr. N. Yoshinaga for valuable discussions. This work was supported by the Grant-in-Aid on priority area "Soft Matter Physics" from the Ministry of Education, Culture, Sports, Science and Technology (MEXT) of Japan and The Next Generation of Physics, Spun from Universality and Emergence.

APPENDIX A

Here, we derive the relation between the coefficients $c_{\ell m}$ in Eq. (18) and the tensor S_{ij}. Let us consider the following elliptic-pancake-type deformation:

$$\delta R(\theta,\phi) = \zeta Y_2^0(\theta,\phi) + \eta \frac{Y_2^2(\theta,\phi) + Y_2^{-2}(\theta,\phi)}{2}, \tag{A1}$$

where $\zeta = c_{20}$ and $\eta = 2c_{22} = 2c_{2-2}$. This definition of η should not be confused with the one given by Eq. (47). The unit vectors $\boldsymbol{n}^{(1)} = (0,0,1)$, $\boldsymbol{n}^{(2)} = (0,1,0)$, and $\boldsymbol{n}^{(3)} = (1,0,0)$ represent the direction of the above shape. We rotate the system successively, first, ψ' about the z axis, and then, $d\theta'$ about the y axis, and, finally, $d\phi'$ about the z axis where $d\theta'$ and $d\phi'$ are infinitesimal and the higher orders $O[(d\theta')^2]$ and $O[(d\phi')^2]$ are ignored. By the successive rotations, the unit vectors are transformed as

$$\boldsymbol{n}^{(1)} = (d\theta, d\theta\, d\phi, 1), \tag{A2}$$

$$\boldsymbol{n}^{(2)} = (-\sin\psi' - \cos\psi' d\phi, \cos\psi' - \sin\psi' d\phi, \sin\psi' d\theta), \tag{A3}$$

$$\boldsymbol{n}^{(3)} = (\cos\psi' - \sin\psi' d\phi, \sin\psi' + \cos\psi' d\phi, -\cos\psi' d\theta). \tag{A4}$$

Here, the order $d\theta\, d\phi$ is retained in Eq. (A2) to make the noncommutability around the y and z axes explicit. From Eq. (25), together with Eqs. (A2)–(A4), one obtains

$$S_{11} = q_2 \sin^2\psi' + q_3 \cos^2\psi' + 2(q_2 - q_3)\sin\psi'\cos\psi' d\phi, \tag{A5}$$

$$S_{12} = -(q_2 - q_3)\sin\psi'\cos\psi' + (q_2 - q_3)(\sin^2\psi' - \cos^2\psi')d\phi, \tag{A6}$$

$$S_{13} = (q_1 - q_2\sin^2\psi' - q_3\cos^2\psi')d\theta - (q_2 - q_3)\cos\psi'\sin\psi' d\theta\, d\phi, \tag{A7}$$

$$S_{22} = q_2\cos^2\psi' + q_3\sin^2\psi' - 2(q_2 - q_3)\sin\psi'\cos\psi' d\phi, \tag{A8}$$

$$S_{23} = (q_2 - q_3)\sin\psi'\cos\psi' d\theta + (q_1 - q_2\sin^2\psi' - q_3\cos^2\psi')d\theta\, d\phi. \tag{A9}$$

Next, we consider the operator $\hat{L} = (1 - d\phi\, L_z)(1 - d\theta\, L_y)\exp(-\psi' L_z)$ where

$$L_y = \cos\phi\frac{\partial}{\partial\theta} - \frac{\cos\theta}{\sin\theta}\sin\phi\frac{\partial}{\partial\phi}, \tag{A10}$$

$$L_z = \frac{\partial}{\partial\phi}. \tag{A11}$$

We operate $\hat{L}$ at both sides of Eq. (A1) to obtain

$$c_{22} = \frac{\eta}{2}\cos 2\psi' + \frac{\eta}{2i}\sin 2\psi' + \frac{\eta}{i}\cos 2\psi' d\phi\eta \sin 2\psi' d\phi, \tag{A12}$$

$$c_{21} = 3\zeta\sqrt{\frac{1}{6}}d\theta - \frac{\eta}{2}\cos 2\psi' d\theta - \frac{\eta}{2i}\sin 2\psi' d\theta + 3\frac{\zeta}{i}\sqrt{\frac{1}{6}}d\theta\, d\phi - \frac{\eta}{2i}\cos 2\psi' d\theta\, d\phi + \frac{\eta}{2}\sin 2\psi' d\theta\, d\phi, \tag{A13}$$

$$c_{20} = \zeta, \tag{A14}$$

$$c_{2-1} = 3\zeta\sqrt{\frac{1}{6}}d\theta - \frac{\eta}{2}\cos 2\psi' d\theta + \frac{\eta}{2i}\sin 2\psi' d\theta - 3\frac{\zeta}{i}\sqrt{\frac{1}{6}}d\theta\, d\phi + \frac{\eta}{2i}\cos 2\psi' d\theta\, d\phi + \frac{\eta}{2}\sin 2\psi' d\theta\, d\phi, \tag{A15}$$

$$c_{2-2} = \frac{\eta}{2}\cos 2\psi' - \frac{\eta}{2i}\sin 2\psi' - \frac{\eta}{i}\cos 2\psi' d\phi - \eta\sin 2\psi' d\phi. \tag{A16}$$

where $c_{\ell m}$ have been defined as the coefficients in Eq. (18). In these derivations, we have used the formulas

$$\frac{d}{d\theta}P_\ell^m(\cos\theta) = m\frac{\cos\theta}{\sin\theta}P_\ell^m(\cos\theta) - P_\ell^{m+1}(\cos\theta) = (\ell + m)(\ell - m + 1)P_\ell^{m-1}(\cos\theta) - m\frac{\cos\theta}{\sin\theta}P_\ell^m(\cos\theta), \tag{A17}$$

$$P_\ell^{m+2}(\cos\theta) = 2(m+1)\frac{\cos\theta}{\sin\theta}P_\ell^{m+1}(\cos\theta) - (\ell - m)(\ell + m + 1)P_\ell^m(\cos\theta), \tag{A18}$$

Comparing Eqs. (A5)–(A9) and (A12)–(A16) and rescaling as $(q_2 + q_3)/(2\zeta) = -1$ and $(q_2 - q_3)/(2\eta) = -\sqrt{3/2}$, one obtains Eq. (26).

APPENDIX B

In this appendix, we describe the details of the derivation of the time-evolution equation of the center of mass $\boldsymbol{\rho}$. From

Eq. (27), the value w of the inhibitor v at the interface of the domain is given by

$$w = w_{(0)} + w_{(1)} + w_{(2)} + w_{(3)}, \tag{B1}$$

where

$$w_{(0)} = \int_{\tilde{q}} G_q H_q(t) e^{i\boldsymbol{q}\cdot\boldsymbol{R}(\theta,\phi)}, \tag{B2}$$

$$w_{(1)} = w_{(11)} + w_{(12)} = i\int_{\tilde{q}} (\boldsymbol{q}\cdot\dot{\boldsymbol{\rho}}) G_q^2 H_q(t) e^{i\boldsymbol{q}\cdot\boldsymbol{R}(\theta,\phi)} - \int_{\tilde{q}} G_q^2 \frac{\partial H_q(t)}{\partial t} e^{i\boldsymbol{q}\cdot\boldsymbol{R}(\theta,\phi)}, \tag{B3}$$

$$w_{(2)} = w_{(21)} + w_{(22)} + w_{(23)} = -i\int_{\tilde{q}} (\boldsymbol{q}\cdot\ddot{\boldsymbol{\rho}}) G_q^3 H_q(t) e^{i\boldsymbol{q}\cdot\boldsymbol{R}(\theta,\phi)} - \int_{\tilde{q}} (\boldsymbol{q}\cdot\dot{\boldsymbol{\rho}})^2 G_q^3 H_q(t) e^{i\boldsymbol{q}\cdot\boldsymbol{R}(\theta,\phi)} + \int_{\tilde{q}} G_q^3 \frac{\partial^2 H_q(t)}{\partial t^2} e^{i\boldsymbol{q}\cdot\boldsymbol{R}(\theta,\phi)}, \tag{B4}$$

$$w_{(3)} = -i\int_{\tilde{q}} (\boldsymbol{q}\cdot\dot{\boldsymbol{\rho}})^3 G_q^4 H_q(t) e^{i\boldsymbol{q}\cdot\boldsymbol{R}(\theta,\phi)}. \tag{B5}$$

We have dropped terms having a factor $\dot{\boldsymbol{\rho}}\dot{H}$ in Eq. (B4) and $\dot{\boldsymbol{\rho}}\dot{\boldsymbol{\rho}}\dot{H}$ and the term with $\ddot{\boldsymbol{\rho}}$ in Eq. (B5). Substituting Eq. (17) into Eq. (29), one obtains, up to the first order of δR,

$$H_q(t) = H_q^{(0)} + H_q^{(1)}, \tag{B6}$$

where

$$H_q^{(0)} = \frac{4\pi R_0^2}{q} j_1(qR_0), \qquad H_q^{(1)} = 4\pi R_0^2 \sum_{\ell,m} (-i)^\ell c_{\ell m}(t)\, j_\ell(qR_0) Y_\ell^m(\theta_q,\phi_q). \tag{B7}$$

The spherical Bessel function $j_\ell(x)$ is defined by

$$j_\ell(x) = x^\ell \left(-\frac{d}{x\,dx}\right)^\ell \frac{\sin x}{x}. \tag{B8}$$

The following formulas have been used:

$$e^{i\boldsymbol{q}\cdot\boldsymbol{r}} = 4\pi \sum_{\ell,m} i^\ell j_\ell(qr) Y_\ell^{m*}(\theta_q,\phi_q) Y_\ell^m(\theta,\phi), \tag{B9}$$

$$\int_0^\pi d\theta\, \sin\theta \int_0^{2\pi} d\phi\, Y_{\ell'}^{m'*}(\theta,\phi) Y_\ell^m(\theta,\phi) = \delta_{\ell'\ell}\delta_{m'm}, \tag{B10}$$

$$\frac{2\ell+1}{x} j_\ell(x) = j_{\ell-1}(x) + j_{\ell+1}(x), \tag{B11}$$

$$j_\ell'(x) = \frac{\ell}{x} j_\ell(x) - j_{\ell+1}(x). \tag{B12}$$

When the interface velocity is low, one can expand the left hand side of Eq. (13) in the power of τc. Substituting Eq. (12) into Eq. (13), one obtains, up to the third order terms,

$$\tfrac{1}{2}(\tau V - \varepsilon K - L) - \tfrac{1}{16}(\tau V - \varepsilon K - L)^3 = 1 - 2p - 2w. \tag{B13}$$

In order to derive the time-evolution equation for $\boldsymbol{\rho}$, we operate $1/\Omega \int d\omega\, \boldsymbol{R}(\omega)$ for both sides of Eq. (B13). Since the Lagrange multiplier L is independent of angles θ and ϕ for a spherical domain, one has $\int d\omega\, \boldsymbol{R}(\omega) L = \int d\omega\, \boldsymbol{R}(\omega) L^3 = \int d\omega\, \boldsymbol{R}(\omega) V^2 L = 0$. Furthermore, since it will be shown that $L \sim O(\dot{\boldsymbol{\rho}}^2)$, from Eq. (C8) in Appendix C, one may ignore $\int d\omega\, \boldsymbol{R}(\omega) V L^2$ up to the third order of $\dot{\boldsymbol{\rho}}$. It is also noted that $\int d\omega\, \boldsymbol{R}(\omega) K(\omega) = 0$ up to the first order of δR since the modes c_{1m} are excluded in Eq. (18). The term $\varepsilon V K$ and the higher order terms with respect to ε are ignored. As a result, we drop $\varepsilon K + L$ in the third term on the left hand side of Eq. (B13).

The zeroth order terms in Eq. (B13) that represent a motionless spherical domain are written as

$$-\frac{\varepsilon}{R_0} + 1 - 2p - 2\int_{\tilde{q}} G_q H_q^{(0)}(t) e^{i\boldsymbol{q}\cdot\boldsymbol{R}_0(\theta,\phi)} = 0, \tag{B14}$$

with $\boldsymbol{R}_0 = R_0 \boldsymbol{e}_r$. The Lagrange multiplier L has been absorbed into the constant p. Equation (B14) gives us the static radius R_0 of the spherical domain as a function of the parameter p [8]. By adding operation $1/\Omega \int d\omega\, \boldsymbol{R}(\omega)$ to Eq. (B13), one obtains the following equation up to the leading order:

$$\frac{\tau}{2}\dot{\boldsymbol{\rho}} - \frac{3\tau^3}{80}\dot{\boldsymbol{\rho}}|\dot{\boldsymbol{\rho}}|^2 = -2\boldsymbol{w}, \tag{B15}$$

where

$$\boldsymbol{w} = \boldsymbol{w}_{(11)} + \boldsymbol{w}_{(21)} + \boldsymbol{w}_{(3)}, \tag{B16}$$

with

$$\boldsymbol{w}_{(11)} = \frac{i}{\Omega}\int d\omega\, \boldsymbol{R}(\omega) \int_{\tilde{q}} (\boldsymbol{q}\cdot\dot{\boldsymbol{\rho}}) G_q^2 H_q(t) e^{i\boldsymbol{q}\cdot\boldsymbol{R}(\omega)}, \tag{B17}$$

$$\boldsymbol{w}_{(21)} = -\frac{i}{\Omega}\int d\omega\, \boldsymbol{R}(\omega) \int_{\tilde{q}} (\boldsymbol{q}\cdot\ddot{\boldsymbol{\rho}}) G_q^3 H_q(t) e^{i\boldsymbol{q}\cdot\boldsymbol{R}(\omega)}, \tag{B18}$$

$$\boldsymbol{w}_{(3)} = -\frac{i}{\Omega}\int d\omega\, \boldsymbol{R}(\omega) \int_{\tilde{q}} (\boldsymbol{q}\cdot\dot{\boldsymbol{\rho}})^3 G_q^4 H_q(t) e^{i\boldsymbol{q}\cdot\boldsymbol{R}(\omega)}. \tag{B19}$$

The integral over ω in Eqs. (B17)–(B19) can be carried out up to the first order with respect to δR as

$$\frac{i}{\Omega}\int d\omega\, \boldsymbol{R}(\omega) e^{i\boldsymbol{q}\cdot\boldsymbol{R}(\omega)} = \boldsymbol{A}_q^{(0)} + \boldsymbol{A}_q^{(1)} = -\frac{3}{q} j_1(qR_0)\boldsymbol{q} + \frac{3}{R_0^2}\sum_{\ell,m} i^\ell c_{\ell m} \times Y_\ell^m(\theta_q,\phi_q) \frac{\partial}{\partial \boldsymbol{q}} [qR_0 j_{\ell-1}(qR_0) - (\ell-1) j_\ell(qR_0)]. \tag{B20}$$

Substituting Eqs. (B6) and (B20) into Eqs. (B17)–(B19), one obtains

$$\boldsymbol{w}_{(11)} = \boldsymbol{w}_{(11)}^{(0)} + \boldsymbol{\delta w}_{(11)} = -\frac{2R_0^2}{\pi}\dot{\boldsymbol{\rho}}\int_0^\infty dq\, q^2 G_q^2 j_1(qR_0)^2 + \boldsymbol{\delta w}_{11}, \tag{B21}$$

$$\boldsymbol{w}_{(21)} = \frac{2R_0^2}{\pi}\ddot{\boldsymbol{\rho}}\int_0^\infty dq\, q^2 G_q^3 j_1(qR_0)^2, \tag{B22}$$

$$\boldsymbol{w}_{(3)} = \frac{6R_0^2}{5\pi}\dot{\boldsymbol{\rho}}|\dot{\boldsymbol{\rho}}|^2\int_0^\infty dq\, q^4 G_q^4 j_1(qR_0)^2. \tag{B23}$$

From Eqs. (B17) and (B20), $\boldsymbol{\delta w}_{(11)}$ is given up to the order of $O(\dot{\boldsymbol{\rho}} c_{\ell m})$ by

$$\boldsymbol{\delta w}_{(11)} \equiv \boldsymbol{\delta w}^{(1)}_{(11)} + \boldsymbol{\delta w}^{(2)}_{(11)} = \int_{\tilde{q}} (\boldsymbol{q}\cdot\dot{\boldsymbol{\rho}}) G_q^2 H_q^{(1)} \boldsymbol{A}_q^{(0)} + \int_{\tilde{q}} (\boldsymbol{q}\cdot\dot{\boldsymbol{\rho}}) G_q^2 H_q^{(0)} \boldsymbol{A}_q^{(1)}. \tag{B24}$$

The first term $\delta w^{(1)}_{(11,i)}$ $(i = x,y,z)$ is written as

$$\delta w^{(1)}_{(11,i)} = \dot{\rho}_j M^{(1)}_{ji}, \tag{B25}$$

where

$$M^{(1)}_{11} = -12\pi R_0^2 \sum_{\ell,m} i^{-\ell} c_{\ell m} \times \int_{\tilde{q}} \frac{q_x^2}{q} G_q^2 Y_\ell^m(\theta_q,\phi_q) j_1(qR_0) j_\ell(qR_0) = a_1 \left[\sqrt{\frac{3}{2}} (c_{22} + c_{2-2}) - c_{20} \right], \tag{B26}$$

$$M^{(1)}_{12} = -12\pi R_0^2 \sum_{\ell,m} i^{-\ell} c_{\ell m} \times \int_{\tilde{q}} \frac{q_x q_y}{q} G_q^2 Y_\ell^m(\theta_q,\phi_q) j_1(qR_0) j_\ell(qR_0) = a_1 \sqrt{\frac{3}{2}} i (c_{22} - c_{2-2}), \tag{B27}$$

$$M^{(1)}_{13} = -12\pi R_0^2 \sum_{\ell,m} i^{-\ell} c_{\ell m} \times \int_{\tilde{q}} \frac{q_x q_z}{q} G_q^2 Y_\ell^m(\theta_q,\phi_q) j_1(qR_0) j_\ell(qR_0) = a_1 \sqrt{\frac{3}{2}} (c_{21} + c_{2-1}), \tag{B28}$$

$$M^{(1)}_{22} = -12\pi R_0^2 \sum_{\ell,m} i^{-\ell} c_{\ell m} \times \int_{\tilde{q}} \frac{q_y^2}{q} G_q^2 Y_\ell^m(\theta_q,\phi_q) j_1(qR_0) j_\ell(qR_0) = a_1 \left[-\sqrt{\frac{3}{2}} (c_{22} + c_{2-2}) - c_{20} \right], \tag{B29}$$

$$M^{(1)}_{23} = -12\pi R_0^2 \sum_{\ell,m} i^{-\ell} c_{\ell m} \times \int_{\tilde{q}} \frac{q_y q_z}{q} G_q^2 Y_\ell^m(\theta_q,\phi_q) j_1(qR_0) j_\ell(qR_0) = a_1 \sqrt{\frac{3}{2}} i (c_{21} - c_{2-1}), \tag{B30}$$

with the symmetry relation $M^{(1)}_{ij} = M^{(1)}_{ji}$. The constant a_1 is given by

$$a_1 = \frac{R_0^2}{\sqrt{5\pi^3}} \int_0^\infty dq\, q^3 G_q^2 j_1(qR_0) j_2(qR_0). \tag{B31}$$

Here, we have used the relations,

$$\int_0^\pi d\theta\, \sin\theta P_n^m(\cos\theta) P_\ell^m(\cos\theta) = \frac{2(n+m)!}{(n-m)!(2n+1)!} \delta_{\ell n}. \tag{B32}$$

It should be noted that, because of the factors $q_i q_j$ in Eqs. (B26)–(B30), only modes c_{2m} contribute to $M^{(1)}_{ij}$.

The second term in Eq. (B24) can be written by using Eq. (B20) as

$$\delta w^{(2)}_{(11,i)} = \dot{\rho}_j M^{(2)}_{ji}, \tag{B33}$$

where

$$M^{(2)}_{ij} = \frac{3}{R_0^2} \sum_{\ell,m} i^\ell c_{\ell m} \int_{\tilde{q}} q_i G_q^2 H_q^{(0)} \frac{\partial}{\partial q_j} \{ Y_\ell^m(\theta_q,\phi_q) \times [qR_0 j_{\ell-1}(qR_0) - (\ell-1) j_\ell(qR_0)] \} = -\frac{3}{R_0^2} \sum_{\ell,m} i^l c_{\ell m} \int_{\tilde{q}} Y_\ell^m(\theta_q,\phi_q) [qR_0 j_{\ell-1}(qR_0) - (\ell-1) j_\ell(qR_0)] \frac{q_i q_j}{q} \frac{\partial}{\partial q} \left(G_q^2 H_q^{(0)} \right). \tag{B34}$$

In the derivation of the second equality, we have used the fact $c_{00} = 0$, which comes from the domain area conservation. Each of the components is readily written as

$$M^{(2)}_{11} = a_2 \left[\sqrt{\frac{3}{2}} (c_{22} + c_{2-2}) - c_{20} \right], \tag{B35}$$

$$M^{(2)}_{12} = a_2 \sqrt{\frac{3}{2}} i (c_{22} - c_{2-2}), \tag{B36}$$

$$M^{(2)}_{13} = a_2 \sqrt{\frac{3}{2}} (c_{21} + c_{2-1}), \tag{B37}$$

$$M^{(2)}_{22} = a_2 \left[-\sqrt{\frac{3}{2}} (c_{22} + c_{2-2}) - c_{20} \right], \tag{B38}$$

$$M^{(2)}_{23} = a_2 \sqrt{\frac{3}{2}} i (c_{21} - c_{2-1}), \tag{B39}$$

where $M^{(2)}_{ij} = M^{(2)}_{ji}$. The constant a_2 is given by

$$a_2 = \frac{1}{\sqrt{5\pi^3}} \int_0^\infty dq\, q^3 [qR_0 j_1(qR_0) - j_2(qR_0)] \times \frac{\partial}{\partial q} \left[\frac{1}{q} G_q^2 j_1(qR_0) \right]. \tag{B40}$$

Equation (32) has been obtained from these results.

APPENDIX C

In this appendix, we derive the time-evolution equation for S_{ij}. Expanding Eq. (12) up to the first order of δR and

substituting Eqs. (23) and (24) into Eq. (12), one obtains

$$\tau \sum_{\ell,m} \dot{c}_{\ell m} Y_\ell^m(\theta,\phi) = -\frac{\varepsilon}{R_0^2} \sum_{\ell,m} (\ell+2)(\ell-1) c_{\ell m} Y_\ell^m(\theta,\phi) - 4\delta w + L, \tag{C1}$$

where $\delta w = w - w_0$ with w_0, the value of w for a spherical domain. We have used the fact that $\tau\, dc(w_0)/dw_0 = -4$ as obtained from Eq. (13).

Since the tensor S_{ij} consists of c_{2m} as shown by Eq. (26), we derive the time-evolution equations of c_{2m}. Only the three terms in Eqs. (B2)–(B4) contribute to the $\ell = 2$ modes,

$$\delta w = \delta w_{(0)} + \delta w_{(1)} + \delta w_{(2)}, \tag{C2}$$

where

$$\delta w_{(0)} = \int_{\tilde{q}} G_q H_q(t) e^{i\boldsymbol{q}\cdot\boldsymbol{R}(\omega)} - \int_{\tilde{q}} G_q H_q^{(0)}(t) e^{i\boldsymbol{q}\cdot\boldsymbol{R}_0(\omega)}, \tag{C3}$$

$$\delta w_{(1)} = -\int_{\tilde{q}} G_q^2 \frac{dH_q(t)}{dt} e^{i\boldsymbol{q}\cdot\boldsymbol{R}(\omega)}, \tag{C4}$$

$$\delta w_{(2)} = -\int_{\tilde{q}} (\boldsymbol{q}\cdot\dot{\boldsymbol{\rho}})^2 G_q^3 H_q(t) e^{i\boldsymbol{q}\cdot\boldsymbol{R}(\omega)}. \tag{C5}$$

We have ignored the term with $\partial^2 H_q/\partial t^2$, which produces $\ddot{c}_{\ell m}$ and is of higher order in Eq. (38). From Eqs. (29) and (C3)–(C5), one obtains

$$\delta w_{(0)} = \frac{2}{\pi} \sum_{\ell,m} A_\ell c_{\ell m} Y_\ell^m(\theta,\phi), \tag{C6}$$

$$\delta w_{(1)} = -\frac{2}{\pi} \sum_{\ell,m} B_\ell \dot{c}_{\ell m} Y_\ell^m(\theta,\phi), \tag{C7}$$

$$\begin{aligned}\delta w_{(2)} = {} & -\frac{2}{3\pi} D_0 |\dot{\boldsymbol{\rho}}|^2 + \frac{4}{5}\sqrt{\frac{5}{\pi}} D_1 \Bigg[\sqrt{\frac{1}{6}} (\dot{\rho}_x - i\dot{\rho}_y)^2 Y_2^2(\theta,\phi) \\ & + \sqrt{\frac{1}{6}} (\dot{\rho}_x + i\dot{\rho}_y)^2 Y_2^{-2}(\theta,\phi) + \sqrt{\frac{2}{3}} (\dot{\rho}_x - i\dot{\rho}_y)\dot{\rho}_z Y_2^1(\theta,\phi) \\ & + \sqrt{\frac{2}{3}} (\dot{\rho}_x + i\dot{\rho}_y)\dot{\rho}_z Y_2^{-1}(\theta,\phi) \\ & - \frac{1}{3}(\dot{\rho}_x^2 + \dot{\rho}_y^2 - 2\dot{\rho}_z^2) Y_2^0(\theta,\phi) \Bigg],\end{aligned} \tag{C8}$$

where

$$A_\ell = R_0^2 \int_0^\infty dq\, q^2 G_q [j_\ell(qR_0)^2 - j_1(qR_0)^2], \tag{C9}$$

$$B_\ell = R_0^2 \int_0^\infty dq\, q^2 G_q^2 j_\ell(qR_0)^2, \tag{C10}$$

$$D_\ell = R_0^2 \int_0^\infty dq\, q^3 G_q^3 j_\ell(qR_0) j_{\ell+1}(qR_0). \tag{C11}$$

It is noted that the first term in $\delta w_{(2)}$ contains an $\ell = 0$ mode proportional to $\dot{\boldsymbol{\rho}}^2$, which should be absorbed into the Lagrange multiplier L in Eq. (C1).

Adding operation $\int d\theta\, d\phi\, \sin\theta Y_2^{m*}(\theta,\phi)$ to both sides of Eq. (C1) yields, for $m = 0,\ \pm 1$, and ± 2,

$$\tau \dot{c}_{2m} = -\frac{4\varepsilon}{R_0^2} c_{2m} - 4\,\delta w_{2m}, \tag{C12}$$

where δw_{2m} is given by

$$\delta w_{2m} = \int_0^\pi d\theta\, \sin\theta \int_0^{2\pi} d\phi\, Y_2^{m*}(\theta,\phi) \delta w(\theta,\phi). \tag{C13}$$

Since the tensor S_{ij} is given by Eq. (26), Eq. (38) is derived from Eqs. (C12) and (C13).

[1] L. M. Pismen, *Patterns and Interfaces in Dissipative Dynamics* (Springer, Berlin, 2006).
[2] H.-G. Purwins *et al.*, Adv. Phys. **59**, 485 (2010).
[3] K. Krischer and A. Mikhailov, Phys. Rev. Lett. **73**, 3165 (1994).
[4] J. E. Pearson, Science **261**, 189 (1993).
[5] K. J. Lee, W. D. McCormick, J. E. Pearson, and H. L. Swinney, Nature (London) **369**, 215 (1994).
[6] V. Petrov, S. K. Scott, and K. Showalter, Philos. Trans. R. Soc. London, Ser. A **347**, 631 (1994).
[7] Y. Hayase and T. Ohta, Phys. Rev. Lett. **81**, 1726 (1998).
[8] T. Ohta, M. Mimura, and R. Kobayashi, Physica D **34**, 115 (1989).
[9] T. Ohta, J. Kiyose, and M. Mimura, J. Phys. Soc. Jpn. **66**, 1551 (1997).
[10] T. Ohta, Physica D **151**, 61 (2001).
[11] S. I. Ei, M. Mimura, and M. Nagayama, Physica D **165**, 176 (2002).
[12] Y. Nishiura, T. Teramoto, and K. Ueda, Chaos **15**, 047509 (2005).
[13] T. Ohta, T. Ohkuma, and K. Shitara, Phys. Rev. E **80**, 056203 (2009).
[14] T. Ohta and T. Ohkuma, Phys. Rev. Lett. **102**, 154101 (2009).
[15] T. Teramoto, K. Suzuki, and Y. Nishiura, Phys. Rev. E **80**, 046208 (2009).
[16] T. Hiraiwa, M. Y. Matsuo, T. Ohkuma, T. Ohta, and M. Sano, Europhys. Lett. **91**, 20001 (2010).
[17] T. Ohkuma and T. Ohta, Chaos **20**, 023101 (2010).
[18] Y. Itino, T. Ohkuma, and T. Ohta, J. Phys. Soc. Jpn. **80**, 033001 (2011).
[19] A. Shapere and F. Wilczek, Phys. Rev. Lett. **58**, 2051 (1987).
[20] H. Boukellal, O. Campas, J.-F. Joanny, J. Prost, and C. Sykes, Phys. Rev. E **69**, 061906 (2004).
[21] T. Hiraiwa, K. Shitara, and T. Ohta, Soft Matter **7**, 3083 (2011).
[22] D. Armbruster, J. Guckenheimer, and P. Holmes, Physica D **29**, 257 (1988).
[23] D. Armbruster, J. Guckenheimer, and P. Holmes, SIAM J. Appl. Math. **49**, 676 (1989).
[24] S. Koga and Y. Kuramoto, Prog. Theor. Phys. **63**, 106 (1980).
[25] B. Kerner and V. V. Osipov, Sov. Phys. Usp. **32**, 101 (1989).
[26] T. Ohta, A. Ito, and A. Tetsuka, Phys. Rev. A **42**, 3225 (1990).
[27] T. Ohta and K. Kawasaki, Macromolecules **19**, 2621 (1986).

[28] J. Rinzel and D. Terman, SIAM J. Appl. Math. **42**, 1111 (1982).
[29] T. Ohta, Ann. Phys. **158**, 31 (1984).
[30] L. G. Fel, Phys. Rev. E **52**, 702 (1995).
[31] A. Ye. Rednikov, Y. S. Ryazantsev and M. G. Velarde, Phys. Fluids **6**, 451 (1994).
[32] A. S. Mikhailov and K. Showalter, Phys. Rep. **425**, 79 (2006).
[33] M. M. Hanczyc, T. Toyota, T. Ikegami, N. Packard, and T. Sugawara, J. Am. Chem. Soc. **129**, 9386 (2007).
[34] T. Toyota, N. Maru, M. M. Hanczyc, T. Ikegami, and T. Sugawara, J. Am. Chem. Soc. **131**, 5012 (2009).
[35] W. L. Zeile, F. Zhang, R. B. Dickinson, and D. L. Purich, Cell Motil. Cytoskeleton **60**, 121 (2005).
[36] H. C. Crenshaw, Am. Zool. **36**, 608 (1996).
[37] V. B. Shenoy, D. T. Tambe, A. Prasad, and J. A. Theriot, Proc. Natl. Acad. Sci. USA **104**, 8229 (2007).
[38] B. M. Friedrich and F. Juelicher, Proc. Natl. Acad. Sci. USA **104**, 13256 (2007).
[39] M. Tarama and T. Ohta (unpublished).